Acta Mechanica Solida Sinica, Vol. 21, No. 3, June, 2008 ISSN 0894-9166
Published by AMSS Press, Wuhan, China. DOI: 10.1007/s10338-008-0829-y

ACTIVE CONTROL OF A FLEXIBLE CANTILEVER PLATE WITH MULTIPLE TIME DELAYS*

Longxiang Chen Ji Pan Guoping Cai

(*Department of Engineering Mechanics, Shanghai Jiaotong University, Shanghai* 200240*, China*)

Received 27 March 2008, revision received 22 June 2008

ABSTRACT Active control of a flexible cantilever plate with multiple time delays is investigated using the discrete optimal control method. A controller with multiple time delays is presented. In this controller, time delay effect is incorporated in the mathematical model of the dynamic system throughout the control design and no approximations and assumptions are made in the controller derivation, so the system stability is easily guaranteed. Furthermore, this controller is available for both small time delays and large time delays. The feasibility and efficiency of the proposed controller are verified through numerical simulations in the end of this paper.

KEY WORDS flexible cantilever plate, multiple time delays, discrete optimal control

I. INTRODUCTION

It is well known that time delay inevitably exists in active control systems. Many factors, such as measurement of system variables, calculation of controller and processes for actuators to build up required control force, may result in the non-synchronization of control force. Time delay may cause degradation of control efficiency, or even renders system instability[1]. So far, the time delay problem is mainly investigated in mathematics and control systems and most studies are focused on stability and maximum time delay for stability of time-delay systems. In dynamics and control of time-delay systems, Hu and Wang[2,3] surveyed the recent advances. Xu et al.[4] proposed the perturbation-incremental scheme (PIS) for delay-induced weak or high-order resonant double Hopf bifurcation and dynamics arising from bifurcation of nonlinear systems with delayed feedback. Xu and Chung[5] investigated the mechanism of action of time delay in a non-autonomous system and *dead island* phenomenon was firstly found. For active control of structures, some treating methods were proposed to deal with time delay, such as the method of Taylor series expansion and the technique of phase shift[6,7]. But these two methods are only available for very small time delay. Recently, Cai[8] proposed a new controller with time delay. This controller has the ability of memory function in all time regions and it may be used to deal with both small time delay and large time delay. The treating methods mentioned above for eliminating the negative effect of time delay are the so-called time-delay elimination technique or time-delay compensation technique. Its main action is to eliminate or weaken the negative effect of time delay on control efficiency. On the other hand, some studies in recent decades have shown that voluntary introduction of delays can also benefit the control. Utilizing time delay to compose a delayed feedback control loop may be used to improve control performance or system stability. For example, in nonlinear dynamics, it is very effective to use time delay to control chaotic motions[9]. In structural

* Project supported by the National Natural Science Foundation of China (Nos. 10772112 and 10472065), the Key Project of Ministry of Education of China (No. 107043) and the Specialized Research Fund for the Doctoral Program of Higher Education of China (No. 20070248032).

control area, Hosek and Olgac[10] developed a time-delay resonator that may be used for vibration control of structures. In robotics area, Cai and Lim[11] designed a delayed feedback controller for a flexible manipulator and this controller may obtain better control effectiveness than control design with no time delay. In control system of pipes conveying fluid, time delay may be utilized to improve steady critical speed of liquid flowing[12]. Time delay may be also used to improve system stability[3]. The studies above involving the active utilization of time delay are the so-called time-delay utilization technique or delayed feedback control method. Although today many effects have been made on the time-delay techniques, there are still many problems remaining to be deeply studied. For example, majority of the existing studies on the time-delay controller only considered single time delay. In other words, all actuators used in structures are assumed to have the same delay. For large or complex flexible structures, such as large-scale flexible plate, more than one actuator is often used for vibration suppression of the plate. All the actuators possibly exhibit different delays due to the different capabilities of actuators. This case is referred to as multiple time delays. For controller design with multiple time delays, to the authors' knowledge, there are seldom any studies up to now.

In this paper, active control of a flexible cantilever plate with multiple time delays is studied, where controller is designed using the discrete optimal control method and piezoelectric patches are used as actuators. A processing method for multiple time delays is presented. The effect of time delay on control performance and the effectiveness of the proposed control design are both verified through numerical simulations.

II. MOTION EQUATIONS

Transverse vibration of a flexible cantilever plate is considered, as shown in Fig.1. Based on the Kirchhoff-Love hypothesis, the free vibration equation of the two-dimensional rectangular plate is[13]

$$D_p(\frac{\partial^4}{\partial x^4}+2\frac{\partial^4}{\partial x^2\partial y^2}+\frac{\partial^4}{\partial y^4})w(x,y,t)+\rho_p h\frac{\partial^2 w(x,y,t)}{\partial t^2}=0 \tag{1}$$

where $w(x,y,t)$ represents the transverse displacement of the point (x,y) at the moment t; $D_p = E_p h^3/[12(1-\nu_p^2)]$ is the flexural rigidity; E_p is the Young's modulus; ν_p is the Poisson's ratio; h is the thickness of the plate; ρ_p is the density of the plate material.

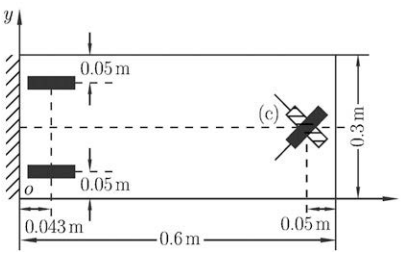

Fig. 1. Locations of PZT actuators on the plate.

Piezoelectric (PZT) patches are used as actuators. The bending moments, m_x and m_y, and the torsional moment m_{xy} produced by the PZT actuator may be written as[13]

$$m_x = m_y = C_0^i\varepsilon_{pe}^i[H(x-x_{1i})-H(x-x_{2i})][H(y-y_{1i})-H(y-y_{2i})] \tag{2}$$

$$m_{xy} = C_0^i\varepsilon_{pe6}^i[H(x-x_{1i})-H(x-x_{2i})][H(y-y_{1i})-H(y-y_{2i})] \tag{3}$$

where $H(\cdot)$ represents the unit Heaviside (step) function; (x_{1i},y_{1i}) and (x_{2i},y_{2i}) are the lower-left and upper-right coordinates of the i-th PZT actuator in the oxy coordinate system, respectively; $\varepsilon_{pe}^i = d_{31}^i V_i/h_{ai}$ and $\varepsilon_{pe6}^i = d_{36}^i V_i/h_{ai}$ are the resultant strains of the i-th PZT actuator; d_{31}^i and d_{36}^i are the piezoelectric material strain constants; V_i is the applied voltage on the i-th PZT actuator; h_{ai} is the thickness of the i-th PZT actuator. The parameter C_0^i represents the mechanical-electrical coupling coefficient between the i-th PZT actuator and the plate, and is given by[13]

$$C_0^i = -\frac{2}{3}\frac{1+\nu_{pei}}{1-\nu_p}\cdot\frac{E_p h_p^2 P_i}{1+\nu_p-(1+\nu_{pei})P_i},\quad P_i = -\frac{E_{pei}}{E_p}\cdot\frac{1-\nu_p^2}{1-\nu_{pei}^2}\cdot\frac{3h_{ai}h_p(2h_p+h_{ai})}{2(h_p^3+h_{ai}^3)+3h_p h_{ai}^2} \tag{4}$$

where E_{pei} and ν_{pei} represent the Young's modulus and Poisson's ratio of the PZT actuator, respectively; h_p is the half thickness of the plate.

The inner moments of the two-dimensional plate are specified by

$$M_x = -D_p\left(\frac{\partial^2 w}{\partial x^2} + \nu_p\frac{\partial^2 w}{\partial y^2}\right),\ M_y = -D_p\left(\frac{\partial^2 w}{\partial y^2} + \nu_p\frac{\partial^2 w}{\partial x^2}\right),\ M_{xy} = -\left(1-\nu_p\right)D_p\left(\frac{\partial^2 w}{\partial x\partial y}\right) \tag{5}$$

Neglect mass and stiffness effects of the piezoelectric material on system dynamics. Using the classical thin plate theory, the equation of motion with material damping can be described as

$$\frac{\partial^2(M_x - m_x)}{\partial x^2} + 2\frac{\partial^2(M_{xy} - m_{xy})}{\partial x\partial y} + \frac{\partial^2(M_y - m_y)}{\partial y^2} - C_s\frac{\partial w}{\partial t} - \rho_p h\frac{\partial^2 w}{\partial t^2} = 0 \tag{6}$$

where C_s is the structural damping operator.

Assume that N_a actuators are installed on the plate. Substituting Eqs.(2), (3) and (5) into Eq.(6), the equation of motion becomes

$$\begin{aligned} D_p\nabla^4 w + C_s\dot{w} + \rho_p h\ddot{w} + \sum_{i=1}^{N_a}\big\{ & C_0^i\varepsilon_{pe}^i[\delta'(x-x_{1i}) - \delta'(x-x_{2i})][H(y-y_{1i}) - H(y-y_{2i})] \\ & + C_0^i\varepsilon_{pe}^i[H(x-x_{1i}) - H(x-x_{2i})][\delta'(y-y_{1i}) - \delta'(y-y_{2i})] \\ & + 2C_0^i\varepsilon_{pe6}^i[\delta(x-x_{1i}) - \delta(x-x_{2i})][\delta(y-y_{1i}) - \delta(y-y_{2i})]\big\} = 0 \end{aligned} \tag{7}$$

where $\nabla^2 = \partial^2/\partial x^2 + 2(\partial^2/\partial x\partial y) + \partial^2/\partial y^2$ and $\delta(\cdot)$ is the Dirac delta function.

Assume that the control forces produced by the N_a actuators exhibit different delays. The motion equation of the plate with time delays can be expressed as

$$\begin{aligned} D_p\nabla^4 w + C_s\dot{w} + \rho_p h\ddot{w} + \sum_{i=1}^{N_a}\Bigg\{ & C_0^i\frac{d_{31}^i}{h_{ai}}[\delta'(x-x_{1i}) - \delta'(x-x_{2i})][H(y-y_{1i}) - H(y-y_{2i})] \\ & + C_0^i\frac{d_{31}^i}{h_{ai}}[H(x-x_{1i}) - H(x-x_{2i})][\delta'(y-y_{1i}) - \delta'(y-y_{2i})] \\ & + 2C_0^i\frac{d_{36}^i}{h_{ai}}[\delta(x-x_{1i}) - \delta(x-x_{2i})][\delta(y-y_{1i}) - \delta(y-y_{2i})]\Bigg\} V_i(t-\lambda_i) = 0 \end{aligned} \tag{8}$$

where λ_i is the delayed time of the i-th PZT actuator, $i = 1, \cdots, N_a$.

The transverse displacement $w(x, y, t)$ of the plate can be expressed as a time-dependent weighted sum of assumed spatial mode shape functions, given by

$$w(x, y, t) = \sum_{m=1}^{\infty}\sum_{n=1}^{\infty} W_{mn}(x, y)\ \eta_{mn}(t) \tag{9}$$

where the subscripts m and n denote the (m, n)-th mode of vibration; W_{mn} and η_{mn} represent the modal function and the modal coordinate, respectively.

The analytical solution of modal function of the plate can not be obtained directly, so modal trial function method is often used to express the modal functions approximately. For the cantilever plate, assume that the (m, n)-th modal function W_{mn} are products of free-free beam modes, $Y_n(y)$, in the chordwise direction and clamed-free beam modes, $X_m(x)$, in the spanwise direction. They can be given by[13]

$$W_{mn}(x, y) = X_m(x)Y_n(y) \tag{10}$$

The expressions of $X_m(x)$ and $Y_n(y)$ may be found in Ref.[13].

In controller design, N_a actuators are used to control the first N_a modes of the plate, i.e., $mn = N_a$. Using the orthogonality of the modal function of cantilever plates, the controlled mode equation may be written as

$$\ddot{\boldsymbol{\Phi}}(t) + \boldsymbol{C}\dot{\boldsymbol{\Phi}}(t) + \boldsymbol{K}\boldsymbol{\Phi}(t) = \sum_{i=1}^{N_a}\boldsymbol{H}_i V_i(t-\lambda_i) \tag{11}$$

where $\boldsymbol{C} = \mathrm{diag}(2\zeta_{11}\omega_{11}, \cdots, 2\zeta_{mn}\omega_{mn})$ and $\boldsymbol{K} = \mathrm{diag}(\omega_{11}^2, \cdots, \omega_{mn}^2)$ are both $N_a \times N_a$ matrices; $\boldsymbol{\Phi}(t) = \{\eta_{11}, \cdots, \eta_{mn}\}^{\mathrm{T}}$ and $\boldsymbol{H}_i = \boldsymbol{M}^{-1}\{\mathrm{piezo}_{11}^i, \cdots, \mathrm{piezo}_{mn}^i\}^{\mathrm{T}}$ are both $N_a \times 1$ vectors, the superscript T denotes the transpose of a matrix or vector; $\boldsymbol{M}$ is the modal mass matrix; the coefficients piezo_{mn}^i of the PZT actuator are given by[13]

$$\begin{aligned}\mathrm{piezo}_{mn}^i = -\Bigg\{ & C_0^i \frac{d_{31}^i}{h_{ai}}[X_m'(x_{2i}) - X_m'(x_{1i})] \int_{y_{1i}}^{y_{2i}} Y_n(y)\mathrm{d}y \\ & + C_0^i \frac{d_{31}^i}{h_{ai}}[Y_n'(y_{2i}) - Y_n'(y_{1i})] \int_{x_{1i}}^{x_{2i}} X_m(x)\mathrm{d}\,x \\ & + 2C_0^i \frac{d_{36}^i}{h_{ai}}[X_m(x_{2i}) - X_m(x_{1i})][Y_n(y_{2i}) - Y_n(y_{1i})]\Bigg\} \end{aligned} \tag{12}$$

III. DISCRETIZATION AND STANDARDIZATION OF MODAL EQUATIONS

The time delay λ_i can be written as

$$\lambda_i = l_i T - \bar{m}_i \quad (i = 1, ..., N_a) \tag{13}$$

where T is the data sampling period, $l_i > 1$ is a positive integer and $0 \le \bar{m}_i < T$. It is pointed out in Ref.[14] that time delay has small effects on control performance and can be ignored in control design if time delay is smaller than the data sampling period T. Time delay affects control system only when it is larger than T. So $\lambda_i > T$ is considered in this paper.

In the state-space representation, Eq.(11) becomes

$$\dot{\boldsymbol{Z}}(t) = \boldsymbol{A}\boldsymbol{Z}(t) + \sum_{i=1}^{N_a} \boldsymbol{B}_i V_i(t - \lambda_i) \tag{14}$$

where $\boldsymbol{Z}(t) = \begin{Bmatrix} \boldsymbol{\Phi}(t) \\ \dot{\boldsymbol{\Phi}}(t) \end{Bmatrix}$ is a $2N_a \times 1$ state vector; $\boldsymbol{A} = \begin{bmatrix} \boldsymbol{0} & \boldsymbol{I} \\ -\boldsymbol{K} & -\boldsymbol{C} \end{bmatrix}$ is a $2N_a \times 2N_a$ system matrix and $\boldsymbol{B}_i = \begin{Bmatrix} \boldsymbol{0} \\ \boldsymbol{H}_i \end{Bmatrix}$ is a $2N_a \times 1$ vector.

The analytical solution of Eq.(14) may be written as[8, 14]

$$\boldsymbol{Z}(t) = \mathrm{e}^{\boldsymbol{A}(t-t_0)}\boldsymbol{Z}(t_0) + \sum_{i=1}^{N_a} \int_{t_0}^{t} \mathrm{e}^{\boldsymbol{A}(t-\tau)}\boldsymbol{B}_i V_i(\tau - \lambda_i)\,\mathrm{d}\tau \tag{15}$$

Zero-order holder is used in the structure, i.e.,

$$V_i(t) = V_i(k), \quad kT \le t < (k+1)T \tag{16}$$

Let $t_0 = kT$ and $t = (k+1)T$, Eq.(15) becomes

$$\boldsymbol{Z}(k+1) = \mathrm{e}^{\boldsymbol{A}T}\boldsymbol{Z}(k) + \sum_{i=1}^{N_a} \int_{kT}^{(k+1)T} \mathrm{e}^{\boldsymbol{A}[(k+1)T-\tau]}\boldsymbol{B}_i V_i(\tau - \lambda_i)\,\mathrm{d}\tau \tag{17}$$

By variable substitution $\eta = (k+1)T - \tau$, Eq.(17) becomes

$$\boldsymbol{Z}(k+1) = \mathrm{e}^{\boldsymbol{A}T}\boldsymbol{Z}(k) + \sum_{i=1}^{N_a} \int_{0}^{T} \mathrm{e}^{\boldsymbol{A}\eta}\boldsymbol{B}_i V_i[(k+1)T - l_i T + \bar{m}_i - \eta]\,\mathrm{d}\eta \tag{18}$$

Consider $\bar{m}_i = 0$ in Eq.(13), namely time delay is integer times of the data sampling period. Substituting Eq.(16) into Eq.(18) and using $\bar{m}_i = 0$, we have

$$\boldsymbol{Z}(k+1) = \boldsymbol{F}\,\boldsymbol{Z}(k) + \sum_{i=1}^{N_a} \boldsymbol{G}_i V_i(k - l_i) \tag{19}$$

where $\boldsymbol{F}=\mathrm{e}^{\boldsymbol{A}T}$ is a $2N_a\times 2N_a$ matrix and $\boldsymbol{G}_i=\int_0^T \mathrm{e}^{\boldsymbol{A}\tau}\mathrm{d}\tau\,\boldsymbol{B}_i$ is a $2N_a\times 1$ vector, $i=1,\cdots,N_a$.

Equation (19) is a time-delay difference equation. Next, consider the standardization of this equation. Augment the state variables in Eq.(19) as

$$\begin{aligned} Z_{2N_a+1}(k)&=V_1(k-l_1)\\ &\vdots\\ Z_{2N_a+l_1}(k)&=V_1(k-1)\\ &\vdots\\ Z_{2N_a+\sum\limits_{i=1}^{N_a-1}l_i+1}(k)&=V_{N_a}(k-l_{N_a})\\ &\vdots\\ Z_{2N_a+\sum\limits_{i=1}^{N_a}l_i}(k)&=V_{N_a}(k-1) \end{aligned} \tag{20}$$

and define a new state vector as

$$\bar{\boldsymbol{Z}}(k)=\left\{\boldsymbol{Z}(k),\quad Z_{2N_a+1}(k),\quad\cdots,\quad Z_{2N_a+\sum\limits_{i=1}^{N_a}l_i}(k)\right\}^{\mathrm{T}} \tag{21}$$

where $\bar{\boldsymbol{Z}}(k)$ is a $(2N_a+\sum\limits_{i=1}^{N_a}l_i)\times 1$ vector. Thus, Eq.(19) can be changed into the following standard discrete form without any explicit time delay

$$\bar{\boldsymbol{Z}}(k+1)=\bar{\boldsymbol{F}}\,\bar{\boldsymbol{Z}}(k)+\bar{\boldsymbol{G}}\boldsymbol{V}(k) \tag{22}$$

where $\bar{\boldsymbol{F}}$ and $\bar{\boldsymbol{G}}$ are $(2N_a+\sum\limits_{i=1}^{N_a}l_i)\times(2N_a+\sum\limits_{i=1}^{N_a}l_i)$ and $(2N_a+\sum\limits_{i=1}^{N_a}l_i)\times N_a$ matrices, respectively; $\boldsymbol{V}(k)$ is an $N_a\times 1$ vector and may be expressed as

$$\boldsymbol{V}(k)=\{V_1(k),\cdots,V_{N_a}(k)\}^{\mathrm{T}},\quad \bar{\boldsymbol{F}}=[\boldsymbol{F}_0,\boldsymbol{F}_1,\cdots,\boldsymbol{F}_{N_a}],\quad \bar{\boldsymbol{G}}=\left[\bar{\boldsymbol{G}}_1,\cdots,\bar{\boldsymbol{G}}_{N_a}\right] \tag{23}$$

where $\boldsymbol{F}_0$ and $\boldsymbol{F}_i$ are $(2N_a+\sum\limits_{i=1}^{N_a}l_i)\times 2N_a$ and $(2N_a+\sum\limits_{i=1}^{N_a}l_i)\times l_i$ matrices, respectively; $\bar{\boldsymbol{G}}_i$ is a $(2N_a+\sum\limits_{i=1}^{N_a}l_i)\times 1$ vector; $\boldsymbol{F}_0$ and $\boldsymbol{F}_i$ $(i=1,\cdots,N_a)$ are component matrices of $\bar{\boldsymbol{F}}$; $\bar{\boldsymbol{G}}_i$ $(i=1,\cdots,N_a)$ are component vectors of $\bar{\boldsymbol{G}}$; given by

$$\boldsymbol{F}_0=\begin{bmatrix}\boldsymbol{F}\\ \boldsymbol{0}\\ \vdots\\ \boldsymbol{0}\\ \boldsymbol{0}\end{bmatrix},\quad \boldsymbol{F}_1=\begin{bmatrix}\boldsymbol{G}_1 & \boldsymbol{0}\cdots\boldsymbol{0}\\ 0 & 1\cdots 0\\ \vdots & \vdots\ \ddots\ \vdots\\ 0 & 0\cdots 1\\ 0 & 0\cdots 0\\ \vdots & \vdots\ \ddots\ \vdots\\ 0 & 0\cdots 0\end{bmatrix},\quad \boldsymbol{F}_i=\begin{bmatrix}\boldsymbol{G}_i & \boldsymbol{0}\cdots\boldsymbol{0}\\ 0 & 0\cdots 0\\ \vdots & \vdots\ \cdots\ \vdots\\ 0 & 0\cdots 0\\ 0 & 1\cdots 0\\ \vdots & \vdots\ \ddots\ \vdots\\ 0 & 0\cdots 1\\ 0 & 0\cdots 0\\ \vdots & \vdots\ \ddots\ \vdots\\ 0 & 0\cdots 0\end{bmatrix}\begin{matrix}\overline{\uparrow}\\ \sum\limits_{j=1}^{i-1}l_j\\ \underline{\downarrow}\end{matrix}\quad(i\neq 1),\quad \bar{\boldsymbol{G}}_i=\begin{bmatrix}\boldsymbol{0}\\ 0\\ \vdots\\ 0\\ 1\\ 0\\ \vdots\\ 0\end{bmatrix}\begin{matrix}\overline{\uparrow}\\ \sum\limits_{j=1}^{i}l_j-1\\ \underline{\downarrow}\end{matrix} \tag{24}$$

For the case $\bar{m}_i\neq 0$ in Eq.(13), the system equation with time delay may be also changed into the standard discrete form as Eq.(22) (for details, see Refs.[8,14]).

IV. DESIGN OF CONTROLLER

In this section, controller design is presented using the discrete optimal control method. To achieve good efficiency, the following continuous performance index is used

$$J=\int_0^{\infty}[\boldsymbol{Z}^{\mathrm{T}}(t)\bar{\boldsymbol{Q}}_1\boldsymbol{Z}(t)+\boldsymbol{V}^{\mathrm{T}}(t)\bar{\boldsymbol{Q}}_2\boldsymbol{V}(t)]\,\mathrm{d}t \tag{25}$$

where $\bar{\boldsymbol{Q}}_1$ is a $2N_a\times 2N_a$ non-negative definite symmetric matrix and $\bar{\boldsymbol{Q}}_2$ is an $N_a\times N_a$ positive definite symmetric matrix. The performance index Eq.(25) is continuous and guarantees good efficiency not only on every sampling point but also between any two adjacent sampling points. However, the discrete performance index can only guarantee good efficiency on every sampling point. Now the task of control design is to design controller for the system Eq.(19) such that the performance index in Eq.(25) attains its minimum. In the previous section, Eq.(19) has been discretized and changed into the standard discrete form without any explicit time delay. Below the performance index Eq.(25) will be discretized and changed to be the function of the augmented state, then the time-delay controller will be presented. Eq.(25) may be written as the following discrete form

$$J=\sum_{k=0}^{\infty}J_k,\quad J_k=\int_{kT}^{(k+1)T}[\boldsymbol{Z}^{\mathrm{T}}(t)\bar{\boldsymbol{Q}}_1\boldsymbol{Z}(t)+\boldsymbol{V}^{\mathrm{T}}(t)\bar{\boldsymbol{Q}}_2\boldsymbol{V}(t)]\,\mathrm{d}t \tag{26}$$

When $kT\le t<(k+1)T$, the solution of Eq.(14) is given by

$$\boldsymbol{Z}(t)=\mathrm{e}^{\boldsymbol{A}(t-kT)}\boldsymbol{Z}(k)+\sum_{i=1}^{N_a}\int_{kT}^{t}\mathrm{e}^{\boldsymbol{A}(t-\tau)}\mathrm{d}\tau\,\boldsymbol{B}_iV_i(k-l_i) \tag{27}$$

Substituting Eq.(27) into Eq.(26) and then arranging the expression, we have

$$J=\sum_{k=0}^{\infty}[\boldsymbol{Z}^{\mathrm{T}}(k)\boldsymbol{Q}_1\boldsymbol{Z}(k)+2\sum_{i=1}^{N_a}\boldsymbol{Z}^{\mathrm{T}}(k)\boldsymbol{Q}_{0i}V_i(k-l_i)+\sum_{i=1}^{N_a}\sum_{j=1}^{N_a}V_i(k-l_i)Q_{ij}V_j(k-l_j)+\boldsymbol{V}^{\mathrm{T}}(k)\boldsymbol{Q}_2\boldsymbol{V}(k)] \tag{28}$$

where $\boldsymbol{Q}_1$ and $\boldsymbol{Q}_{0i}$ are $2N_a\times 2N_a$ and $2N_a\times 1$ matrices, respectively; Q_{ij} is a scalar and $\boldsymbol{Q}_2$ is an $N_a\times N_a$ matrix; given by

$$\begin{aligned}
&\boldsymbol{Q}_1=\textstyle\int_0^T\boldsymbol{F}^{\mathrm{T}}(t)\bar{\boldsymbol{Q}}_1\boldsymbol{F}(t)\,\mathrm{d}t,\quad \boldsymbol{Q}_2=\bar{\boldsymbol{Q}}_2T\\
&\boldsymbol{Q}_{0i}=\left[\textstyle\int_0^T\boldsymbol{F}^{\mathrm{T}}(t)\bar{\boldsymbol{Q}}_1\boldsymbol{G}_{11}(t)\,\mathrm{d}t\right]\boldsymbol{B}_i\quad(i=1,\cdots,N_a)\\
&Q_{ij}=\boldsymbol{B}_i^{\mathrm{T}}\left[\textstyle\int_0^T\boldsymbol{G}_{11}^{\mathrm{T}}(t)\bar{\boldsymbol{Q}}_1\boldsymbol{G}_{11}(t)\,\mathrm{d}t\right]\boldsymbol{B}_j\quad(i,j=1,\cdots,N_a)
\end{aligned} \tag{29}$$

where $\boldsymbol{F}(t)=\mathrm{e}^{\boldsymbol{A}t}$ and $\boldsymbol{G}_{11}(t)=\int_0^t\mathrm{e}^{\boldsymbol{A}\tau}\mathrm{d}\tau$ are both $2N_a\times 2N_a$ matrices.

The performance index Eq.(25) may be rearranged as the following standard form

$$J=\sum_{k=0}^{\infty}[\bar{\boldsymbol{Z}}^{\mathrm{T}}(k)\hat{\boldsymbol{Q}}_1\bar{\boldsymbol{Z}}(k)+\boldsymbol{V}^{\mathrm{T}}(k)\hat{\boldsymbol{Q}}_2\boldsymbol{V}(k)] \tag{30}$$

where $\hat{\boldsymbol{Q}}_1$ and $\hat{\boldsymbol{Q}}_2$ are $(2N_a+\sum_{i=1}^{N_a}l_i)\times(2N_a+\sum_{i=1}^{N_a}l_i)$ and $N_a\times N_a$ matrices, respectively; given by

$$\hat{\boldsymbol{Q}}_1=\begin{bmatrix}
\boldsymbol{Q}_1 & \boldsymbol{Q}_{01} & \mathbf{0}\cdots\boldsymbol{Q}_{0i} & \mathbf{0}\cdots\boldsymbol{Q}_{0N_a} & \mathbf{0}\\
\boldsymbol{Q}_{01}^{\mathrm{T}} & Q_{11} & 0\cdots Q_{1i} & 0\cdots Q_{1N_a} & \mathbf{0}\\
\mathbf{0} & 0 & 0\cdots 0 & 0\cdots 0 & \mathbf{0}\\
\vdots & \vdots & \vdots\ddots\vdots & \vdots\ddots\vdots & \vdots\\
\boldsymbol{Q}_{0i}^{\mathrm{T}} & Q_{i1} & 0\cdots Q_{ii} & 0\cdots Q_{iN_a} & \mathbf{0}\\
\mathbf{0} & 0 & 0\cdots 0 & 0\cdots 0 & \mathbf{0}\\
\vdots & \vdots & \vdots\ddots\vdots & \vdots\ddots\vdots & \vdots\\
\boldsymbol{Q}_{0N_a}^{\mathrm{T}} & Q_{N_a1} & 0\cdots Q_{N_ai} & 0\cdots Q_{N_aN_a} & \mathbf{0}\\
\mathbf{0} & \mathbf{0} & \mathbf{0}\cdots\mathbf{0} & \mathbf{0}\cdots\mathbf{0} & \mathbf{0}
\end{bmatrix},\quad \hat{\boldsymbol{Q}}_2=\bar{\boldsymbol{Q}}_2T \tag{31}$$

Equation (30) is a standard form of performance index. So the next task is to design optimal controller for the system Eq.(22) by minimizing the objective function given by Eq.(30). This controller may be designed using discrete optimal control method, given by[8]

$$\boldsymbol{V}(k) = -\boldsymbol{L}\bar{\boldsymbol{Z}}(k) = -\boldsymbol{L}_1\boldsymbol{Z}(k) - \boldsymbol{L}_2 V_1(k-l_1) - \cdots - \boldsymbol{L}_{l_1+1} V_1(k-1) - \cdots - \boldsymbol{L}_{\sum_{j=1}^{i-1} l_j+2} V_i(k-l_i)$$

$$- \cdots - \boldsymbol{L}_{\sum_{j=1}^{i} l_j+1} V_i(k-1) - \cdots - \boldsymbol{L}_{\sum_{j=1}^{N_a-1} l_j+2} V_{N_a}(k-l_{N_a}) - \cdots - \boldsymbol{L}_{\sum_{j=1}^{N_a} l_j+1} V_{N_a}(k-1) \quad (32)$$

where $\boldsymbol{L}$ is an $N_a \times (2N_a + \sum_{i=1}^{N_a} l_i)$ matrix; $\boldsymbol{L}_1$ is an $N_a \times 2N_a$ matrix; $\boldsymbol{L}_2, \cdots, \boldsymbol{L}_{\sum_{j=1}^{N_a} l_j+1}$ are all $N_a \times 1$ vectors. $\boldsymbol{L}_1$,$\boldsymbol{L}_2, \cdots, \boldsymbol{L}_{\sum_{j=1}^{N_a} l_j+1}$ are component matrices of $\boldsymbol{L}$. Parameter $\boldsymbol{L}$ is given by[8,14]

$$\boldsymbol{L} = [\hat{\boldsymbol{Q}}_2 + \bar{\boldsymbol{G}}^{\mathrm{T}}\boldsymbol{S}\bar{\boldsymbol{G}}]^{-1}\bar{\boldsymbol{G}}^{\mathrm{T}}\boldsymbol{S}\bar{\boldsymbol{F}} \quad (33)$$

where $\boldsymbol{S}$ is a $(2N_a + \sum_{i=1}^{N_a} l_i) \times (2N_a + \sum_{i=1}^{N_a} l_i)$ matrix that is the solution of the following discrete Riccati algebraic equation

$$\boldsymbol{S} = \bar{\boldsymbol{F}}^{\mathrm{T}}[\boldsymbol{S} - \boldsymbol{S}\bar{\boldsymbol{G}}(\hat{\boldsymbol{Q}}_2 + \bar{\boldsymbol{G}}^{\mathrm{T}}\boldsymbol{S}\bar{\boldsymbol{G}})^{-1}\bar{\boldsymbol{G}}^{\mathrm{T}}\boldsymbol{S}]\bar{\boldsymbol{F}} + \hat{\boldsymbol{Q}}_1 \quad (34)$$

We can observe from Eq.(32) that the controller $\boldsymbol{V}(k)$ at the moment kT contains not only the state term $\boldsymbol{Z}(k)$ at this moment, but also some control terms before this moment.

Computations for $\boldsymbol{F}(t)$, $\boldsymbol{G}_{11}(t)$, $\boldsymbol{G}_i$, $\boldsymbol{Q}_1$, $\boldsymbol{Q}_{0i}$ and Q_{ij} may be found in Refs.[8,14]. They are summed up as follows

$$\begin{aligned} &\boldsymbol{G}_{11} = \boldsymbol{I}T + \boldsymbol{O}\boldsymbol{A}, \quad \boldsymbol{D}_0 = \bar{\boldsymbol{Q}}_1\boldsymbol{O} + \boldsymbol{A}^{\mathrm{T}}\boldsymbol{W} \\ &\boldsymbol{F} = \boldsymbol{I} + \boldsymbol{G}_{11}\boldsymbol{A}, \quad \boldsymbol{G}_i = \boldsymbol{G}_{11}\boldsymbol{B}_i \\ &\boldsymbol{Q}_1 = \bar{\boldsymbol{Q}}_1\boldsymbol{G}_{11} + \boldsymbol{A}^{\mathrm{T}}\boldsymbol{D}_0^{\mathrm{T}}, \quad \boldsymbol{Q}_{0i} = \boldsymbol{D}_0\boldsymbol{B}_i \\ &Q_{ij} = \boldsymbol{B}_i^{\mathrm{T}}\boldsymbol{W}\boldsymbol{B}_j \quad (i,j = 1, \cdots, N_a) \end{aligned} \quad (35)$$

where $\boldsymbol{O}$ and $\boldsymbol{W}$ are both $2N_a \times 2N_a$ matrices, given by

$$\begin{aligned} &\boldsymbol{O} = \sum_{k=2}^{\infty} \boldsymbol{O}_k, \quad \boldsymbol{O}_k = \frac{\boldsymbol{A}T}{k}\boldsymbol{O}_{k-1}, \quad \boldsymbol{O}_2 = \frac{T^2}{2}\boldsymbol{I} \\ &\boldsymbol{W} = \sum_{k=2}^{\infty} \boldsymbol{W}_k, \quad \boldsymbol{W}_k = \frac{T}{k+1}(\boldsymbol{A}^{\mathrm{T}}\boldsymbol{W}_{k-1} + \boldsymbol{W}_{k-1}\boldsymbol{A} + \bar{\boldsymbol{Q}}_1\boldsymbol{V}_k + \boldsymbol{V}_k^{\mathrm{T}}\bar{\boldsymbol{Q}}_1), \quad \boldsymbol{W}_2 = \frac{\bar{\boldsymbol{Q}}_1 T^3}{3} \end{aligned} \quad (36)$$

The parameters $\boldsymbol{O}$ and $\boldsymbol{W}$ in Eq.(36) will both converge to constant matrices in limited steps of iterative computation[14].

V. NUMERICAL SIMULATIONS

To demonstrate the effectiveness of the proposed control method, numerical simulations are carried out in this section. Aluminum alloy plate is adopted as the structural model. The length, width and thickness of the rectangle plate are $a = 0.6\,\mathrm{m}$, $b = 0.3\,\mathrm{m}$ and $h = 0.0015\,\mathrm{m}$, respectively, as shown in Fig.1. Material properties of the plate are as follows: Young's elastic modulus is $E_p = 69\,\mathrm{GPa}$, Poisson's ratio is $\nu_p = 0.32$ and density is $\rho_p = 2.7 \times 10^3\,\mathrm{kg/m}^3$. Structural damping ratio of the plate is chosen to be 0.5%. PZT actuators used in this studies have the same size, given by $0.06\,\mathrm{m} \times 0.015\,\mathrm{m} \times 0.0005\,\mathrm{m}$. The material parameters of PZT actuators are as follows: Young's elastic modulus is $E_{pe} = 63\,\mathrm{GPa}$, Poisson's ratio is $\nu_{pe} = 0.35$, piezoelectric strain constants are $d_{31} = 1.75 \times 10^{-10}\,\mathrm{m/V}$ and $d_{36} = 0$.

Locations of PZT actuators are shown in Fig.1. Since the flexible plate considered herein is larger in size, two groups of PZT actuators are used to obtain enough control forces. The first group (denoted by Group I) consists of four PZT patches that are bonded symmetrically to each side of the plate near the clamped end (see Fig.1). The main action of Group I is to control the bending modes of

the plate. The coordinates of the middle points of these four PZT patches are (0.043 m, 0.05 m) and (0.043 m, 0.25 m), respectively, as shown in Fig.1. Assume that these four actuators exhibit the same delayed time, denoted by λ_1. The second group (denoted by Group II) consists of two PZT patches that are bonded anti-symmetrically to each side of the plate near the tip position and their action is to control the torsional modes of the plate. The coordinates of the middle points of these two PZT patches are (0.55 m, 0.15 m). The slope angles of these two actuators with respect to the x-axis direction are 45° and 135°, respectively, as shown in Fig.1. Assume that these two actuators exhibit the same delayed time, denoted by λ_2. In the numerical computation, the sampling period is chosen as $T = 0.01$ s. Assume that the initial condition of plate is $w(0.6,\ 0,\ 0) = 0.02$ m, $\dot{w}(0.6,\ 0,\ 0) = 0$, i.e., the lower-right point of the plate has an initial displacement at zero moment. Under this initial condition, the plate will behave with free vibration. The first two modal frequencies of the plate are 3.4898 Hz and 15.026 Hz, where the first one corresponds to the bending mode and the second one the torsional mode. So the first group of PZT actuators is used to control the first-order bending mode and the second group to control the second-order torsional mode.

PZT materials may bear high voltage up to 2000 V per millimeter. But the electric-field intensity keeps linear relationship with the strain of PZT material only when external electric-field intensity does not exceed 300 V per millimeter. The applied voltage has the relationship, $U = \bar{E}\, h_a$, with the electric-field intensity applied on the PZT material, where U is the applied voltage, $\bar{E}$ the electric-field intensity and h_a is the thickness of the PZT material. Since the thickness of the PZT material adopted in this paper is 0.0005 m, the maximal voltage applied on the PZT material should not exceed ±150 V, thus to guarantee the PZT material working within the linear scope. This may be easily ensured in practice by PZT power amplifier and DSP digital board in fact.

The following case is considered firstly: time delay exists in the system, but it is not compensated in control design, namely the controller designed in the case of no time delay (the non-time-delay controller) is applied for the system with time delay. Assume that all the PZT actuators exhibit the same delayed time, i.e., $\lambda_1 = \lambda_2$. In control design, the gain matrices in Eq.(25) are chosen to be $\bar{\boldsymbol{Q}}_1 = \mathrm{diag}(\,100,\, 100,\, 1,\, 1\,)$ and $\bar{\boldsymbol{Q}}_2 = \mathrm{diag}(\,10^{-8},\, 10^{-8}\,)$. Figure 2 demonstrates the time histories of maximum displacement of the lower-right tip point (i.e., the point of (0.6 m, 0) on the plate) of the plate varying with time delay, where the solid line represents the result using the time-delay controller and the dashed line using the non-time-delay controller to control the system with time delay . It is observed from Fig.2 that the system may suffer from instability at a small time delay $\lambda_1 = \lambda_2 = 0.016$ s if time delay is not compensated. The flexible plate may be effectively controlled by the proposed time-delay controller.

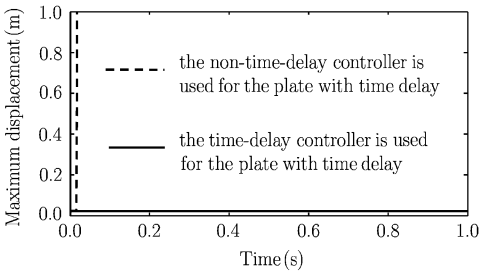

Fig. 2 Maximum response of down-right point of the plate varying with time delay.

Next consider large time delay. The following two cases are considered:
Case 1: λ_1 and λ_2 exist in the two groups of actuators but they are not compensated in control design, namely the non-time-delay controller is used for the system with time delay;
Case 2: λ_1 and λ_2 exist, and the time-delay controller proposed is used for the system.

The gain matrices are chosen to be the same as the above. The case ($\lambda_1 = 0.50$ s, $\lambda_2 = 0.60$ s) is considered, i.e., $l_1 = 50$ and $l_2 = 60$ in Eq.(13). Figures 3(a), (b) and (c) demonstrate the time histories of the lower-right tip point (i.e., the point of (0.6 m, 0) on the plate) and the voltages of the two groups of actuators, where the solid line represents the result using the time-delay controller, the dashed line using the non-time-delay controller to control the system without time delay, the dot-dashed line using the non-time-delay controller to control the system with time delay, and the double dot-dashed line without control for the system. It is observed from Figs.3 that the system may suffer from instability if time delay is not compensated. The flexible plate may be effectively controlled by the proposed time-delay controller. Furthermore, the proposed time-delay controller may achieve almost the same control efficiency as the controller with no time delay.

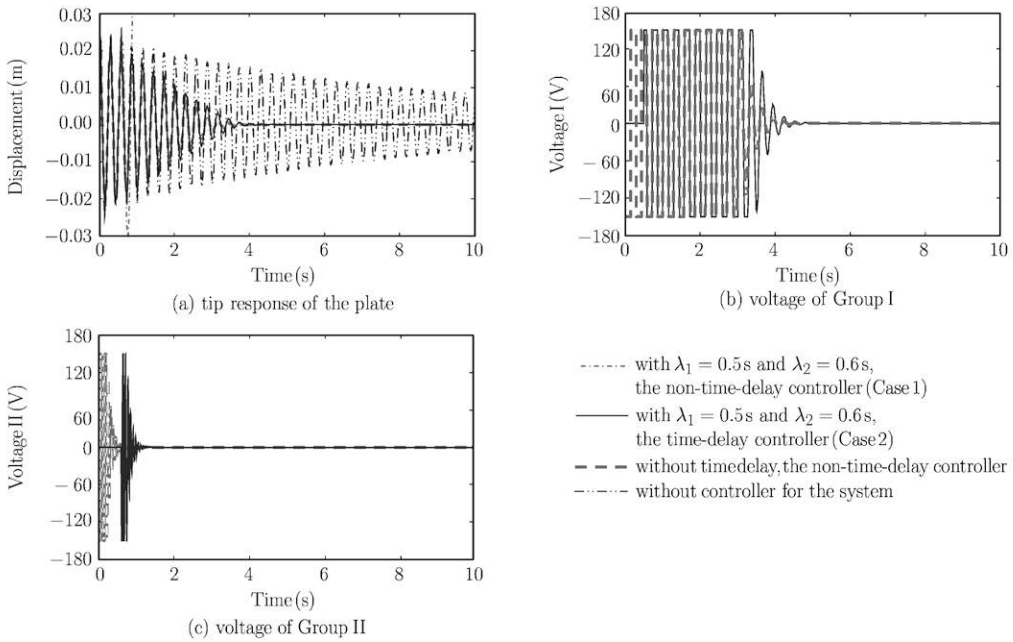

Fig. 3. The time histories of tip response of the plate and the voltages of two groups of PZT actuators.

VI. CONCLUSIONS

In this paper, active control of a flexible cantilever plate with multiple time delays is investigated, where controller is designed using the discrete optimal control method and PZT patches are used as actuators. A processing method for multiple time delays is proposed. Some conclusions can be drawn from this investigation: (1) Time delay in an active control system is an important issue that should be paid more attention. It may render instability of the systems if it is not compensated in control design; (2) The proposed time-delay controller may deal with both small time delay and large time delay. Good control effectiveness may be obtained by this controller; (3) Delayed feedback control is a feasible strategy that may be used for structural control. Under the same control gain matrices, the control effectiveness using the delayed feedback controller is almost the same as that using the controller without time delay.

References

[1] Hu,H.Y., On dynamics in vibration with time delay. *Chinese Journal of Vibration Engineering*, 1997, 10(3): 273-279 (in Chinese).

[2] Hu,H.Y. and Wang,Z.H., Singular perturbation methods for nonlinear dynamic systems with time delays. *Chaos, Solitons and Fractals*, 2007, doi:10.1016/j.chaos.2007.07.048.

[3] Wang,Z.H. and Hu,H.Y., Stabilization of vibration systems via delayed state difference feedback. *Journal of Sound and Vibration*, 2006, 296(1-2): 117-129.

[4] Xu,J., Chung,K.W. and Chan,C.L., An efficient method for studying weak resonant double Hopf bifurcation in nonlinear systems with delayed feedbacks. *SIAM Journal of Applied Dynamical Systems*, 2007, 6(1): 29-60.

[5] Xu,J. and Chung,K.W., Effects of time delayed position feedback on a van der Pol–Duffing oscillator. *Physica D*, 2003, 180: 17-39.

[6] Abdel-Rohman,M., Time-delay effects on active damped structures. *Journal of Engineering Mechanics*, 1987, 113(11): 1709-1719.

[7] Chung,L.L., Reinhorn,A.M. and Soong,T.T., Experiments on active control of seismic structures. *Journal of Engineering Mechanics, ASCE*, 1998, 114(2): 241-256.

[8] Cai,G.P. and Hong,J.Z., Optimal control method for seismically excited building structures with time-delay in control. *Journal of Engineering Mechanics, ASCE*, 2002, 128(6): 602-612.

[9] Xiao,M. and Cao,J.D., Bifurcation analysis and chaos control for Lu system with delayed feedback. *International Journal of Bifurcation and Chaos*, 2007, 17(12): 4309-4322.

[10] Hosek,M. and Olgac,N., A single-step automatic tuning algorithm for the delayed resonator vibration absorber. *IEEE/ASME Transactions on Mechatronics*, 2002, 7(2): 245-255.
[11] Cai,G.P. and Lim,C.W., Optimal tracking control of flexible hub-beam system with time delay. *Multibody System Dynamics*, 2006, 16(4): 331-350.
[12] Yuan,F., Effects of delayed feedback control on stability in the cantilever pipe conveying fluid. *Master dissertation of Tongji University*, 2008 (in Chinese).
[13] Qiu,Z.C., Zhang,X.M., Wu,H.X. and Zhang,H.H., Optimal placement and active vibration control for piezoelectric smart flexible cantilever plate. *Journal of Sound and Vibration*, 2007, 301: 521-543.
[14] Sun,Z.X., Theory and Application of Computer Control. Beijing: Tsinghua University Press, 1989 (in Chinese).